Oligodendrocytes and the role of iron in magnetic susceptibility driven frequency shifts in white matter

Tianyou Xu[1], Sean Foxley[1], and Karla Miller[1]
[1]*Oxford Centre for Functional Magnetic Resonance Imaging of the Brain, University of Oxford, Oxford, Oxfordshire, United Kingdom*

Introduction: The sensitivity of susceptibility-weighted contrast to white matter microstructure is a topic of recent interest. In particular there is increasing evidence that the magnetic susceptibility χ of myelin is sufficiently distinct from intra and extra axonal water to alter the MR signal.[1-6] Previous works aimed at describing the relation between susceptibility-driven properties of white matter and the resultant MR signal have relied on models consisting of only hollow cylinders, which simulate axons and their myelin sheaths.[4-6] While these models benefit from simplicity, they do not capture the full diversity of microstructures present in white matter. Other neuroglia, with distinct magnetic susceptibilities and volumes, may also have significant influence modulating the MR signal. This work extends a geometric model of axonal packing to include the potential contribution of glial cells to susceptibility weighted contrast in white matter.[6] Our results indicate that the volumes occupied by glia, particularly iron-rich oligodendrocytes with their positive susceptibility relative to myelin, could have a significant impact on the underlying proton frequency distributions and the subsequent free induction decay signal magnitude and phase.

Methods: We present a geometric model of white matter that includes both axonal and glial compartments, where our focus for the glial compartment is on iron-rich oligodendrocytes. Axons were assigned a mean radius of 0.5 µm (Gamma distributed with α=3.82 and β=1.26E-7), a mean g-ratio of 0.67 (Gaussian distributed) and a packing density of ~83%.[7] Oligodendrocytes were given radii of 5.5 microns.[8] With said dimensions these glia occupied a volume fraction of 16%, consistent with values in the literature: 10-30%.[9] Oligodendrocytes have the highest iron content of all brain cell types, the predominant form of which is in the non heme storage protein ferritin.[15] We obtained a volume susceptibility shift $\Delta\chi$ of +10 ppm (referenced to CSF) based on ferritin's well studied properties (it holds ~4500 iron atoms, has a radius of 6 nm, a molecular weight of 474 kg/mole and a χ_{volume} of +520 ppm (SI) and concentrations of ferritin in white matter of 2.40 µg/g).[10,11] To include magnetic susceptibility anisotropy in our modeling of myelin, field perturbations were calculated using the Fourier-susceptibility tensor framework.[14] Anisotropic susceptibility χ_a is described by a rank 2 tensor whose diagonal elements represent the longitudinal and perpendicular tensor components of the radial myelin unit.[3,5] Magnetic susceptibility, in complete form, is a summation of both the isotropic and anisotropic components (Eq. 1). A value of -10 ppm was set for both isotropic and anisotropic susceptibility, which is within the range estimated values.[5,13] This implementation allows us to perform field simulations at any desired orientation to B_0; however, to accentuate the susceptibility shift effect, calculations in this work are performed in 2D assuming that the static field (set to 3T) is orthogonal to the plane. Axons are assumed infinite in the third dimension. Specific treatment for fields generated by the oligodendrocytes is detailed in the results section. The sizes of the simulations cover ~50x50 µm. A three-compartment axon model was used to generate the complex signal, described by the signal equation in Eq. 2 where f_n represents all the proton frequencies in compartment n. Other parameters are listed above in the table.

Parameters	Myelin	Intra-Axonal	Extra-Axonal	Oligod.
T2	25 ms	75 ms	75 ms	75 ms
Proton Density	0.5	1	1	1
$\Delta\chi_{isotropic/anisotropic}$	-10 ppm	0	0	+10 ppm (isotropic)

Eq. 1

$$\chi_{ij} = \chi_{iso} I_2 + \chi_a \begin{pmatrix} 1 & 0 & 0 \\ 0 & -\frac{1}{2} & 0 \\ 0 & 0 & -\frac{1}{2} \end{pmatrix}$$

$$S(t) = \sum_{n=1}^{3} \rho_n \, e^{-t/T_{2,n}} \, e^{i\,2\pi\,t\,f_n}$$

Eq. 2

Results: Case A shows the field perturbations of a regular packing of axons, with no oligodendrocytes. Case B simulates a packing in which 16% of the volume is allocated to structures with no susceptibility shift. These voided spaces may represent astrocytes, whose size and volume fractions are comparable to those of oligodendrocytes.[9] Cases C and D incorporate oligodendrocytes of spherical and cylindrical geometries, respectively. Oligodendrocytes have been observed to arrange themselves in rows in white matter.[12] Therefore, in case D we assume that the length of a row of such cells is much greater than its width, allowing us treat these structures as infinite in the third dimension (as with axons). In Case C, analytic formulations for the spherical fields are used. Frequency distributions are obtained by sampling a center FOV, shown by the red circle in Fig A. Each packing yields a distinct asymmetric frequency distribution, shown in figures E through H; these differences are subsequently manifested in their magnitude and phase evolutions (Figures I-J). The intra-axonal peak at -3.78 Hz that is consistent across the four cases affirms the simulated g-ratio (mean of 0.67); this relation has been derived analytically in earlier works.[3,5]

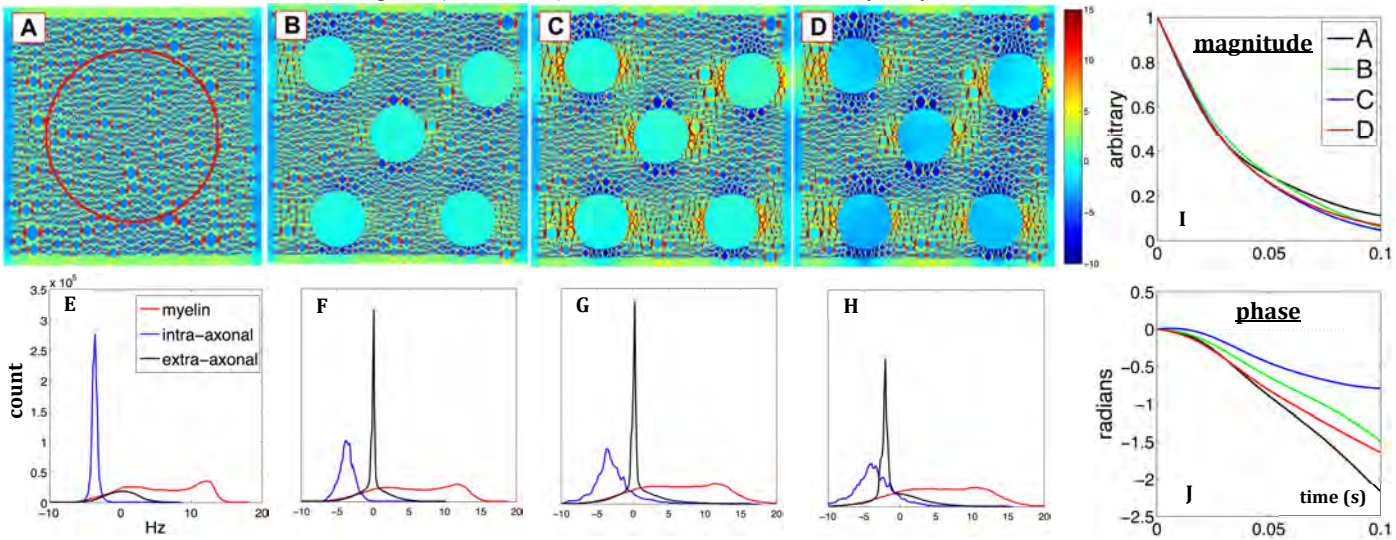

Conclusion: We demonstrate that the incorporation of oligodendrocytes has a significant impact on the underlying frequency distribution and MR signal by virtue of their nontrivial volume fractions and magnetic susceptibility. The inclusion of these structures could therefore be important to accurately characterize the complex relation between white matter properties and the MR signal.

Acknowledgements: University of Oxford's Clarendon Trust Graduate Scholarship and the Wellcome Trust.

Citations: **(1)** Lee et al. Neuroimage 2012. **(2)** Li et al. MRM 2009. **(3)** Sukstanskii et al. MRM 2014. **(4)** Sati et al. Neuroimage 2013. **(5)** Wharton et al. PNAS 2012. **(6)** Chen et al. Neuroimage 2013. **(7)** Barazany et al. Brain 2009. **(8)** Butt A. Neuroglia, Chapter 6 2013. **(9)** Perge et al. The Journal of Neuroscience 2009. **(10)** Schenk J. Med. Phys. 1996 **(11)** Chen et al. Radiology 1989. **(12)** Todorich et al. Glia 2009. **(13)** Lee et al. PNAS 2009. **(14)** Liu C. MRM 2010. **(15)** Wagner et al. Journal of CBFM 2003.